Reliability Assessment of a 5-metre Railway Steel Bridge: A Case Study

Caroline C. de Faria, Túlio N. Bittencourt, Daniel M. Guirardi, André T. Beck

CCF & TNB – Department of Structural and Geotechnical Engineering, University of São Paulo, Av. Prof. Almeida Prado, São Paulo, 05508-900, Brazil
DMG – Institute for Technological Research, Av. Prof. Almeida Prado, São Paulo, 05508-901, Brazil
ATB – Structural Engineering Department, University of São Paulo, Av. Trabalhador São-Carlense, São Carlos, 13566-590, SP, Brazil

Summary

This study presents a reliability analysis of a 5-metre-long railway steel bridge, focusing on the performance of a critical beam. The bridge comprises two I-shaped beams, four diagonal bracings fabricated from angle sections, and two U-shaped cross beams. The applied loads include dead loads, such as the structure's weight, sleepers, rails, guard rails, and connections, along with live loads from trains and wind forces. The aim is to estimate the reliability indices and failure probabilities of the structure, both in its intact state and after the loss of two diagonal bracings, and to identify key parameters. The analysis employs the First-Order Reliability Method and Monte Carlo simulation to account for uncertainties in material properties, geometry, and loading conditions. This methodology provides valuable insights into the bridge's safety performance under various scenarios, offering engineers a framework for making informed decisions from the conceptual design phase onward.

1 INTRODUCTION

Structural design is a multifaceted process influenced by a range of factors, including economic, environmental, political, and social considerations, as well as client specifications, resource availability, standardisation, and implementation feasibility. These factors guide the engineering team in selecting the structural system, stabilisation methods, and the design of component cross-sections and connections. The design process typically follows the limit state method, which includes two main categories: ultimate limit states (ULS), which ensure structural strength, and serviceability limit states (SLS), which address functionality and aesthetics. During the design of steel structures, the primary objective is often to minimise the total steel weight while satisfying all project requirements.

During the calculation phase, computational tools are employed to assist in the design and development of detailed shop, assembly, and field drawings. Although these tools contribute to achieving high accuracy, especially in steel structures, it is crucial to acknowledge inherent uncertainties, such as variations in material properties, geometric dimensions, workmanship, and loads. Deterministic approaches, relying on fixed values, are insufficient to capture these uncertainties. Structural reliability theory provides a more comprehensive framework for assessing and mitigating risks.

Reliability analysis is also useful in the conceptual phase of the project since it helps engineers make informed decisions about the structure's configuration and components. By applying this methodology early on, engineers can optimise the design for both safety and cost-effectiveness.

However, the application of reliability theory is still limited due to challenges such as the lack of specialised software, computational challenges, and a general unfamiliarity among engineers. This article presents a case study on the application of structural reliability methods — specifically the First-Order Reliability Method (FORM) and Monte Carlo simulation — on the design of a 5-metre steel railway bridge. The study focuses on a critical beam of the bridge, analysing the serviceability limit state of vertical deflection and the interaction between flexure and axial force. The analysis includes both an intact bridge and a scenario involving the loss of two diagonal bracings, aiming to estimate failure probabilities and identify the most influential variables.

2 METHODOLOGY

The steel bridge consists of four diagonal bracings (L101.6x12.7), two cross beams (U255x68x12.5x9.5), and two symmetric welded I-profiles (denoted as PS). The terminology for the structural components is as follows: for the angles, the format is L angle width x thickness; for the channels, it is U channel height x flange width x flange thickness x web thickness; and for the I-profile, it is PS height x flange width x flange thickness x web thickness. All dimensions are given in millimetres.

The bridge geometry and the identification of its members are shown in Fig. 1. In this study, the bridge was designed according to Brazilian standards, and then, the reliability analysis was performed on a critical beam (L2), as described in Sections 2.1 and 2.2, respectively.

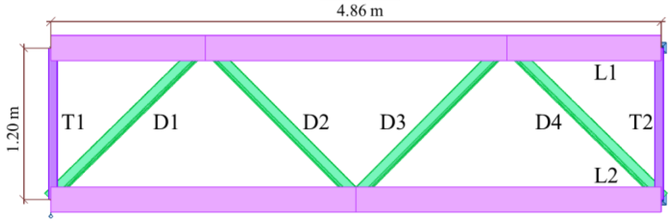

Fig. 1 Bridge geometry and member identification.

2.1 Design according to standards

The structure was designed following the Brazilian guidelines [1]–[4], considering dead loads — including the structure's self-weight, wood sleepers, rails (TR 45), guard rails (TR 37), and connection elements — as well as live loads from the trains (TB 270 from [4]), and wind forces. A dynamic impact factor (φ) of 1.48 was used according to [3]. The structure was modelled using the software Robot Structural Analysis Professional 2024 (Fig. 1), considering bar elements. The train loads were simulated as moving loads.

In load combinations without the train traffic, the wind load was modelled as a distributed force on a single beam (speed = 45 m/s and a statistical factor of 1.11), with an exposed height of 0.76 m and a drag coefficient of 0.63.

When considering simultaneous wind and train loads, loads were applied at the same points as the train's wheel positions (see Fig. 2), with the wind speed set to 25 m/s in line with the recommendations of [5]. In this case, the drag coefficient was 3.73. Additionally, the effect of wind-induced overturning was considered. By modelling the wind acting at the carbody's geometric centre, an equivalent vertical load was calculated. The overturning effect was modelled by increasing the vertical force on one beam and decreasing it on the other (see Fig. 2), considering the lever arm equal to 2.25 m and the metric rail gauge.

Symmetric welded I-profiles with flange width b_f = 200 mm, web thickness t_w = 12.5 mm, and heights d_g in multiples of 100 mm, were evaluated. For the vertical deflection, a limit of $L/600$ due to the train load was considered, where L is the beam length. The lightest profiles meeting these criteria were PS 400x200x31.5x12.5 (132 kg/m), PS 500x200x19x12.5 (105 kg/m), and PS 600x200x16x12.5 (106 kg/m), which showed vertical deflections of 0.81 cm, 0.70 cm, and 0.52 cm, respectively. The critical combination for the ultimate limit states was *1.35 dead load + 1.50 φ.train load + wind*, with the bending moment and the shear force being 525 kN·m and 560 kN, respectively, and the C_b factor for non-uniform bending moment equal to 1.41. The utilization rates of the PS 400, PS 500, and PS 600 profiles were 0.87, 0.94, and 0.83, respectively.

The critical load configurations identified for beam L2 from the moving load model are shown in Fig. 2. In cases (A) and (C) of Fig. 2, the transverse loads simulate the wind acting on the opposite side of the bridge to beam L2. This results in an overturning effect that increases the vertical loads on beam L2. In contrast, in cases (B) and (D), the wind acts on the same side of beam L2, and the vertical load is relieved.

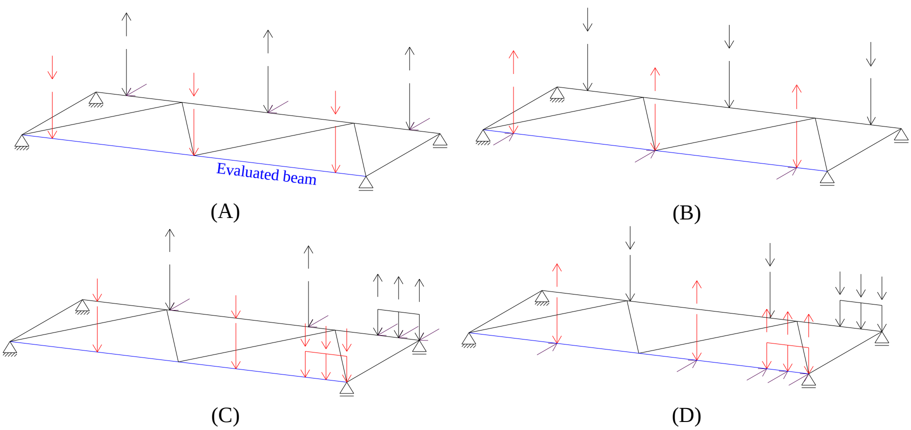

Fig. 2 Critical train and wind loadings' configurations identified for ULS for beam L2.

2.2 Reliability analysis

The reliability analysis was performed focusing on beam L2 (see Figs. 1 and 2), considering the three cross-sections determined in Section 2.1 and the four loading configurations shown in Fig. 2. The First-Order Reliability Method (FORM) and Monte Carlo simulations were implemented using MATLAB. The HLRF and iHLRF optimisation algorithms were used, as detailed in [6]. The transformation steps followed the Nataf Model, with solutions provided in [7]. No correlation was considered between the random variables.

For vertical deflection, Monte Carlo simulations were conducted for comparison. A Latin Hypercube Sampling technique was used to reduce variance, generating a number of samples (n_s) equal to 5 million. Independent samples for normal and lognormal variables were obtained using the Box-Muller algorithm [6].

2.2.1 Random variables

The statistics considered in this study are presented in Table 1. The heights and corresponding flange thicknesses in Table 1 refer to the three cross-sections determined in Section 2.1. The uncertainties in the train load were modelled through coefficients of variation (COV) of 0.10 and 0.15. Additionally, the impact factor was evaluated both as a deterministic value and as a random variable. Thus, three cross-sections, two load scenarios, and two impact factor scenarios were assessed.

Table 1 Distribution, mean, and coefficient of variation (COV) of each random variable.

Description	Symbol	Distrib.	Mean	COV	Unit	Ref
Elastic modulus	E	Lognormal	216,000	0.06	MPa	[6]
Yield strength (A36 steel)	f_y	Normal	335	0.09	MPa	[8]
Profile height	d_g	Normal	40/50/60	0.3/Mean	cm	[8]
Flange thickness	t_f	Normal	3.1428/1.8956/1.5963	0.0477	cm	[8]
Web thickness	t_w	Normal	1.25	0.05/Mean	cm	Adapted from [9]
Max. annual wind speed	W	Gumbel	26.1243	0.2062	m/s	[10]
Locomotive point load	P	Normal	135	0.10/0,15	kN	-
Wagons distributed load	q	Normal	45	0.10/0,15	kN/m	-
Impact factor	φ	Normal	1.479	–/0,10	-	-

2.2.2 Limit state equation for vertical deflection

After evaluating the moving load model, the maximum displacement was identified for the load configuration shown in Fig. 3, with d_a = 2.00 m, d_b = 1.16 m, d_c = 1.00 m, d_d = 0.70 m, and L = 4.86 m. For this configuration, using a limit deflection of L/600, the limit state equation is given by Eq. (1). A total of 12 models were evaluated, considering the three cross-sections determined in Section 2.1, two coefficients of variation for the loads, and two impact factor scenarios.

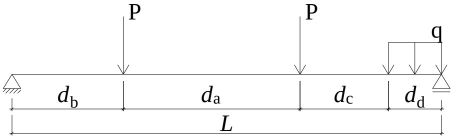

Fig. 3 Critical position identified for vertical deflection considering the TB 270 train loading.

$$g_{\text{deflection}}(E, d_g, t_f, t_w, P, q, \varphi) = \frac{L}{600} - \varphi\,\frac{1}{EI}\left[-\frac{R_a(L/2)^3}{6} + \frac{P(L/2 - d_b)^3}{6} + \frac{CL}{2}\right]$$

where I is the moment of inertia about the x-axis (strong axis), and:

$$R_a = \frac{P}{L}(d_a + 2d_c + 2d_d) + \frac{qd_d^2}{2L} \tag{1}$$

$$C = \frac{R_a L^2}{6} - \left\{\frac{P}{6L}\cdot\left[(L - d_b)^3 + (L - d_a - d_b)^3\right] + \frac{qd_d^4}{24L}\right\}$$

2.2.3 Limit state equation for axial and flexure interaction

In addition to the scenarios described in Section 2.2.1, both intact and damaged states — where diagonals D2 and D3 were removed (see Fig. 1) — were evaluated, totalling 24 models. The general form of the limit state equations analysed for Cases A to D shown in Fig. 2 is given by:

$$g_{N+M}(E, f_y, d_g, t_f, t_w, W, P, q, \varphi) = 1 - \frac{N_{Sk}}{2N_{Rk}} - \left(\frac{M_{x,Sk}}{M_{x,Rk}} + \frac{M_{y,Sk}}{M_{y,Rk}}\right) \tag{2}$$

where N_{Sk}, $M_{x,Sk}$, and $M_{y,Sk}$ represent the calculated axial force and bending moments about the strong and weak axes, respectively, without load factors; and N_{Rk}, $M_{x,Rk}$, and $M_{y,Rk}$ are the corresponding resistances, calculated according to [1], including the C_b factor and without applying resistance factors.

3 RESULTS

3.1 Vertical deflection

The reliability indices for vertical deflections of the PS 400, PS 500, and PS 600 profiles, calculated using FORM, are shown in Fig. 4(a). A comparison of the reliability indices obtained via FORM and the upper and lower bounds from the Monte Carlo simulation is presented in Fig. 4(b). The convergence of the Monte Carlo simulations is illustrated in Fig. 4(c). Additionally, the sensitivity coefficients are displayed in Fig. 5, where the positive sign (+) indicates a random variable for resistance, while the negative sign (-) represents a random variable for load or demand.

As expected, the profile with the largest height and highest moment of inertia, PS 600, exhibits the highest reliability index. However, it is important to note the significant differences in reliability indices among the three profiles. For instance, in the most critical scenario — where the coefficient of variation (COV) of the loads is 0.15, and the COV of the impact factor is 0.10 — the reliability index for PS 400 is β_{FORM} = 0.392, corresponding to a failure probability ($p_{f,FORM}$) of 0.348. In contrast, for the same scenario, PS 600 yields a reliability index of β_{FORM} = 3.063, with a much lower $p_{f,FORM}$ of 0.0011.

It can be observed that an increase in the COV of the load leads to an increase in the point load sensitivity coefficient, causing the reliability index curve to shift downward. Furthermore, the impact factor has a significant effect on the results. When treated as a random variable, the impact factor causes a downward shift in the reliability index curve, with sensitivity coefficients ranging from 0.28 to 0.40. Additionally, the distributed load (q) and geometric properties have a minimal impact on the results. Therefore, the most influential variables are the point load (P), impact factor (φ), and modulus of elasticity (E).

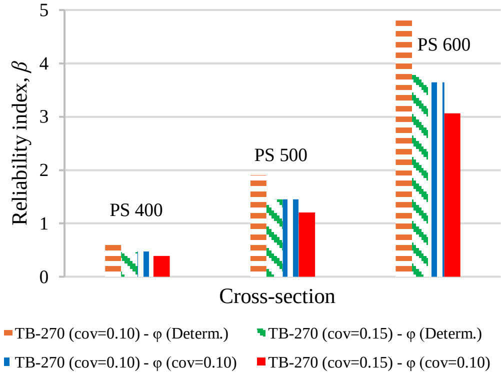

(a)

Cross-section	COV TB-270	β_{FORM}	$\beta_{MC,lower}$	$\beta_{MC,upper}$
PS 400	0.100	0.475	0.505	0.507
PS 500	0.100	1.455	1.480	1.483
PS 600	0.100	3.646	3.665	3.708
PS 400	0.150	0.392	0.427	0.429
PS 500	0.150	1.206	1.238	1.241
PS 600	0.150	3.063	3.090	3.107

(b)

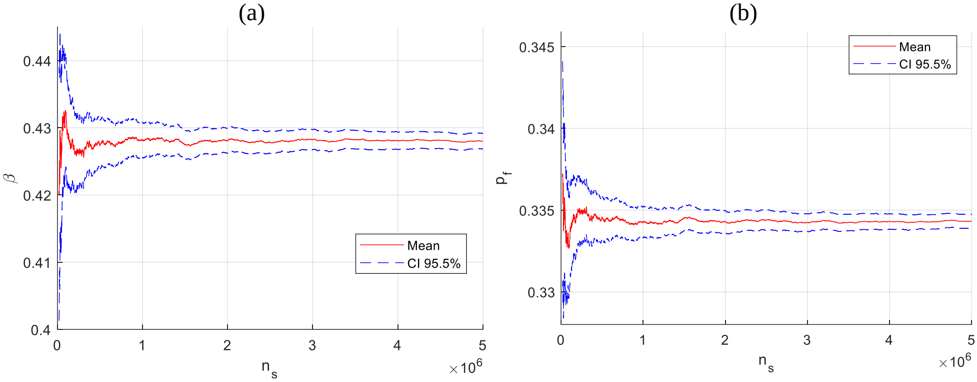

(c)

Fig. 4 (a) Reliability indices for vertical deflection obtained using FORM; (b) comparison between FORM and Monte Carlo results, considering the impact factor as a random variable and (c) convergence of the Monte Carlo simulation for PS 400, $COV_{TB\ 270} = 0.15$ and $COV_{\varphi} = 0.10$.

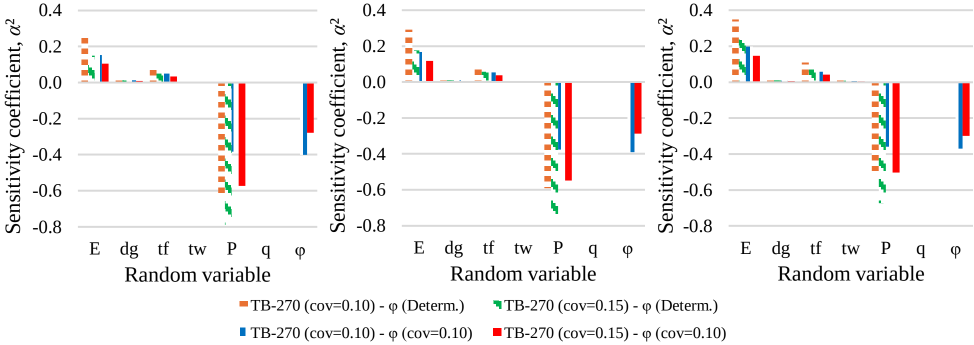

(a) PS 400 (b) PS 500 (c) PS 600

Fig. 5 Sensitivity coefficients determined using FORM.

3.2 Axial and flexure interaction

Out of the 96 limit state equations evaluated, convergence issues were observed in 5 cases. For four of these cases, the issue was resolved by adjusting the standardized parameters of the iHLRF algorithm [11]. This section presents the results for Case A and Case B (see Fig. 2), which are representative of the scenarios investigated.

Results for Case A (Fig. 2) are shown in Fig. 6. For reference, the JCSS reliability limit of 4.4 for the ultimate limit state (ELU) is also displayed, considering normal safety measures and severe failure consequences. In the intact state, all investigated cross-sections met the JCSS limit. However, when the diagonal bracings are removed, the probability of failure increases and only the PS 400 profile met the JCSS limit in all scenarios. The lowest reliability index of 3.51 was observed for the PS 500.

After the removal of the diagonal bracings, the beam's unbraced span doubles, which causes the cross-section's moment resistance about the strong axis to deviate from the plastic moment. This is associated with the redistribution of sensitivity coefficients from f_y to variables such as P, φ, and t_f.

Figure 7 shows the results for Case B (Fig. 2), where the investigated beam experiences a reduction in vertical force but is subjected to bending about the *y*-axis (weak axis). In this case, it can be observed that the damaged state significantly increases the wind sensitivity coefficient. In the intact state, the investigated beam behaves as a continuous beam with three supports, and weak-axis bending is minimal. However, after the intermediate support is lost, the unbraced length doubles, increasing the beam's susceptibility to transverse actions. Comparing the flange sections — the primary elements resisting transverse actions — the PS 400 profile exhibits significantly higher stiffness (200x31.5 mm vs. 200x19 mm and 200x16 mm), explaining its superior reliability indices compared to the PS 500 and PS 600 profiles.

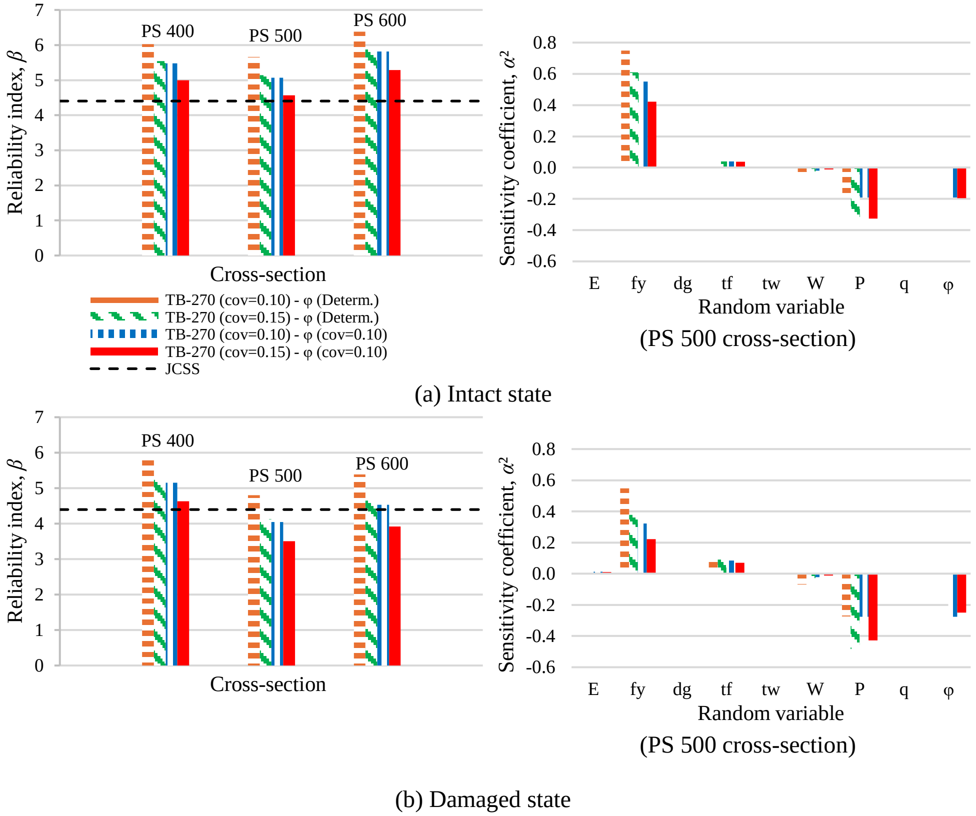

Fig. 6 Case A – Reliability indices and sensitivity coefficients for the axial and flexure interaction in the intact and damaged states.

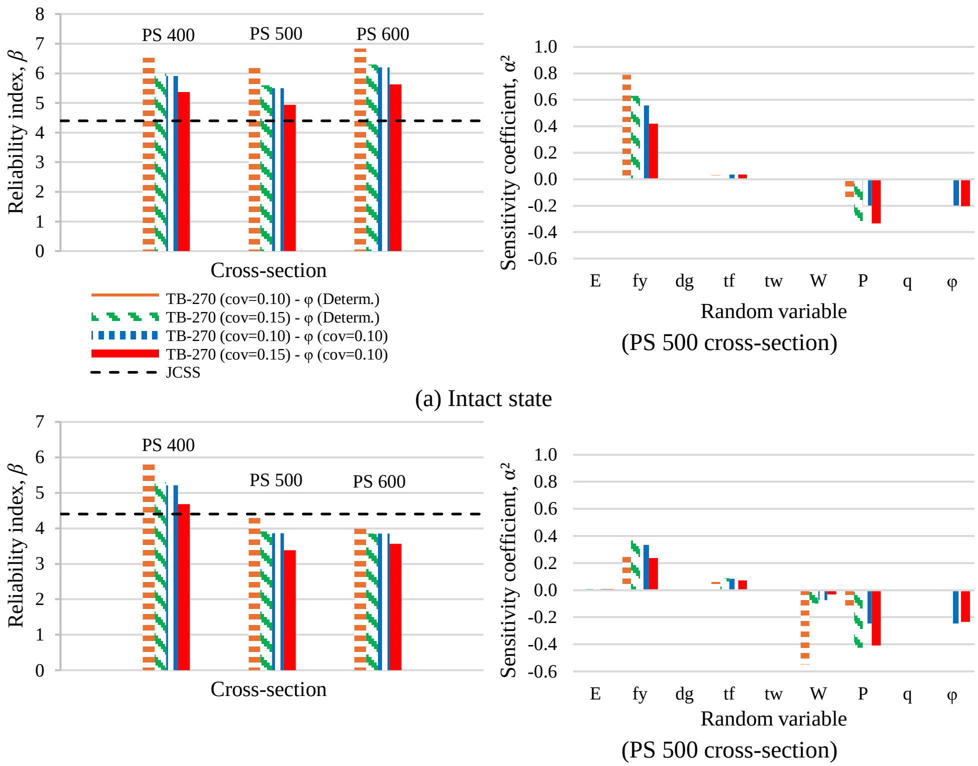

(b) Damaged state

Fig. 7 Case B – Reliability indices and sensitivity coefficients for the axial and flexure interaction in the intact and damaged states.

4 CONCLUSIONS

This study has conducted a structural reliability analysis focusing on a beam of a railway steel bridge. Limit state equations related to vertical deflection and the interaction between axial force and bending moment were evaluated using the FORM transformation method and Monte Carlo simulations. Initially, the structure was designed following the recommendations of [1]. Subsequently, 24 models were assessed using reliability theory, considering intact and damaged configurations; three profiles (PS 400x200x31.5x12.5, PS 500x200x19x12.5, and PS 600x200x16x12.5); coefficients of variation for TB-270 of 0.1 and 0.15, and the analysis of the impact factor as either a deterministic value or a random variable.

For the limit state equation related to vertical deflection, the most relevant variables were P, φ, E, and t_f. The results from FORM and Monte Carlo simulations were in close agreement. The PS 400 profile exhibited the lowest reliability indices, ranging from 0.39 to 0.62, while the PS 600 profile showed the highest values, from 3.06 to 4.82.

For the limit state equations related to the interaction between axial force and bending moment, the most relevant variables were f_y, P, W, φ, and t_f. The PS 400 profile demonstrated the highest reliability indices, ranging from 5.00 to 6.68 in the intact state, and from 4.63 to 5.88 in the damaged state. Conversely, the lowest reliability indices were observed for the PS 500 profile, reaching 3.51 in the damaged state.

The application of reliability theory can help engineers identify optimised geometric configurations and cross-sections starting from the conceptual design phase. For example, in this study, it was observed that none of the cross-sections designed according to the standards outperformed the others in both the ultimate limit state (ULS) and serviceability limit state (SLS). This suggests that the optimal solution for the investigated problem would likely require a PS 500 profile with a larger flange than the one evaluated.

In conclusion, this study underscores the importance of considering uncertainties associated with random variables, such as material properties, structural dimensions, and loading conditions. Future investigations should expand the analysis to include additional loading types and geometric configurations, as well as further explore the combined effects of wind and railway traffic. In particular, given the significance of the variables P and φ, there is a clear need to develop representative statistics for Brazilian railway traffic and establish guidelines for calculating the impact factor. This is especially relevant since the moving load standard [4] was cancelled without replacement in 2015, and unlike that of version [3], the current version [12] no longer includes expressions for calculating the impact factor in railway structures.

Acknowledgements

The first author acknowledges the support from FAPESP (Grant 2023/09449-2).

References

[1] ABNT. NBR 8800:2024. *Design of steel and composite structures for buildings*. Rio de Janeiro, 2024.

[2] ABNT. NBR 6123:2023. *Wind loads on buildings*. Rio de Janeiro, 2023.

[3] ABNT. NBR 7187:2003. *Design of reinforced and prestressed concrete bridges – Procedure*. Rio de Janeiro, 2003.

[4] ABNT. NBR 7189:1985. *Moving loads for structural engineering for railway construction – Procedure*. Rio de Janeiro, 1985.

[5] EUROPEAN UNION. EN 1991-1-4 (2005). *Eurocode 1: Actions on structures - Part 1-4: General actions - Wind actions*. Brussels, 2010.

[6] Beck, A. T. 2024. *Confiabilidade e segurança das estruturas*. Santa Catarina: Orsa Maggiore.

[7] Liu, P. L.; Kiureghian, A. D. 1986. "Multivariate distribution models with prescribed marginals and covariances." *Probabilistic Engineering Mechanics*, 1(2). doi.org/10.1016/0266-8920(86)90033-0.

[8] Santiago, A. *et al*. 2020. "Reliability-based calibration of main Brazilian structural design codes." *Latin American Journal of Solids and Structures*, 17(1):e245. doi.org/10.1590/1679-78255754.

[9] Kala, Z. *et al*. 2009. "Material and geometrical characteristics of structural steels based on statistical analysis of metallurgical products." *Journal of Civil Engineering and Management*, 15(3):299-307. doi.org/10.3846/1392-3730.2009.15.299-307.

[10] Vallis, M. B. 2019. "Brazilian extreme wind climate." PhD Thesis, Federal University of Rio Grande do Sul, Porto Alegre.

[11] Beck, A. T.; Ávila da S. Jr., C. R. 2016. "Strategies for finding the design point under bounded random variables." *Structural Safety*, 58:79-93. doi.org/10.1016/j.strusafe.2015.08.006.

[12] ABNT. NBR 7187:2021. *Design of concrete bridges, viaducts and footbridges*. Rio de Janeiro, 2021.